

# Leveraging Pilot-Scale Data for Real-Time Analysis of Ion Exchange Chromatography

Søren Villumsen<sup>a</sup>, Jesper Frandsen<sup>a</sup>, Jakob Kjøbsted Huusom<sup>a</sup>, Xiaodong Liang<sup>a</sup>, Jens Abildskov<sup>a</sup>

<sup>a</sup> Dept. of Chemical and Biochemical Engineering, Technical University of Denmark, Søltofts Plads, Building 228A, 2800 Kgs. Lyngby, Denmark

\* Corresponding Author: [soevi@kt.dtu.dk](mailto:soevi@kt.dtu.dk)

## ABSTRACT

This study evaluates the potential for computer-aided real-time monitoring and decision-making in pilot-scale ion-exchange chromatography operations using only historical data from the pilot-scale facility. Historical data of flow and conductivity were utilized from students running pilot-scale ion exchanges that resemble industrial ion exchange processes. A Lumped Rate Model (LRM) with a Steric Mass Action (SMA) isotherm was implemented and parameterized to characterize the fixed-bed column. The Discontinuous Galerkin Spectral Element Method (DGSEM), implemented in CADET-Julia, enabled efficient simulation and parameter estimation. Using DGSEM, the LRM with SMA was solved in less time than the sensor measurement frequency. This development allows for the prediction of batch evolution in real time for operators of the ion-exchange column. Despite challenges related to data preprocessing and manual operation inconsistencies, the results demonstrate the feasibility of integrating real-time analysis into pilot-scale operations.

**Keywords:** Ion-exchange chromatography, Real-time analysis, Pilot-scale, Computer-aided, Modelling, DGSEM

## 1. INTRODUCTION

Chromatography constitutes an important part of downstream bio-manufacturing, where it is used to separate valuable products of upstream production. Precise control over chromatographic processes aids in increasing product yield. Current conservative operational strategies sometimes lead to product loss, which may be remediable with real-time process insights [1].

Batch-to-batch variations in feed composition and operating conditions further complicate achieving optimal yields [2]. Improved understanding and monitoring of separation processes could enable operators to account for batch-to-batch variation, increasing yields without sacrificing product quality [2].

The complexity of chromatographic processes arises from their underlying mechanisms, which can be described using partial differential equations (PDEs) that model advection, diffusion, mass transfer, and adsorption. To enable real-time applications involving systems governed by PDEs, fast discretization methods are essential for solving these equations accurately and efficiently.

This study investigates the potential for real-time process analysis using a pilot-scale ion exchange column at the Technical University of Denmark (DTU) pilot facility. For more details on this facility, see [3]. Here, an ion exchange fixed-bed column equipped with sensors is used as a teaching instrument. The column and the exercises run on it resemble operations encountered in industrial ion exchange operations. The system is equipped with sensors that automatically log measurements every two seconds.

There exist historical data sets of these sensor measurements for experiments run by students from 2019 onwards. In this case, students use the data to perform calculations relating to upscaling the process. Beyond this, the data is not employed for other purposes. This has some resemblance to industrial process systems, where sensors are placed on systems for monitoring and quality control purposes, and process optimization using historical data is an afterthought. This study will evaluate whether the fixed-bed column can be characterized solely by historical data and whether such data provides a sufficient foundation for real-time process applications.

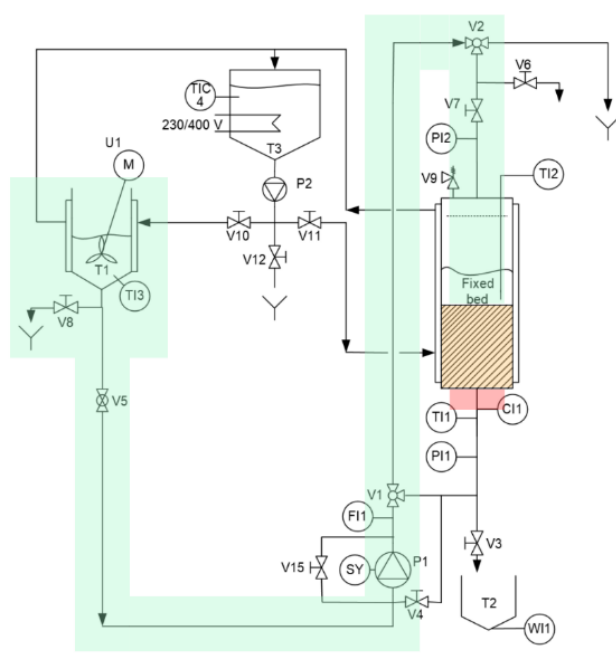


**Figure 1:** (Left) An image of the pilot-scale fixed-bed ion exchange column and (right) P&I diagram for the pilot-scale ion exchange fixed-bed column [8]. The green, orange, and red sections on both the image and the P&I diagram represent the in-flow pipes, the fixed-bed column, and the out-flow pipes, respectively.

## 2. METHODOLOGY

### 2.1 Scoping

There are two subjects of interest in this study. First is the ability to simulate operation of the ion-exchange system based entirely on historical data. The historical data gathered by students was not intended for applications such as those suggested in this study but rather as data to support other investigations. Here, this study investigates the degree to which this data can be repurposed for column characterization and process simulation.

Secondly, the study will investigate if, by using computationally fast numerical schemes, the ion-exchange breakthrough process can be simulated in less time than the measurement frequency of every two seconds. Achieving this would support the development of real-time applications, as the numerical scheme could be solved uniquely for each data point that is gathered. A real-time application of interest in this setting would be the prediction of the breakthrough profile, enabling feedback to the operators of the system as they operate the system.

### 2.2 Experimental Methods

The data used for this study stems from exercises performed by chemical engineering students at DTU [8].

The goal of the exercise is for students to evaluate breakthrough curves during the operation and regeneration of an ion-exchange system, and to determine isotherms and resin properties for scaling up a pilot plant unit.

#### Pilot Plant Setup

The experimental setup features a 10 cm diameter, 1 m tall column occupied by a fixed-bed ion exchange resin. In Figure 1, a piping and instrumentation (P&I) diagram for the system can be seen. The feed solution, stored in a 100 L tank (T1), is pumped through the column. The system includes the following instrumentation:

- Flow-through cell (CI1): Measures conductivity
- Magnetic flow indicator (FI1): Measures flow rate
- Pt100 sensors (TI1 & TI2): Monitor temperature
- Manometer (PI1): Records pressure

Data for time, flow, conductivity, temperature, and pressure are logged automatically every 2 seconds. The resin used is Amberjet 1200 in H-form. The operator must manually control the system by configuring the pump spend and configure valve settings.

#### Experimental Procedure

30 L of 0.1 N  $\text{NaNO}_3$  feed solution is prepared by dissolving  $\text{NaNO}_3$  in water, mixing thoroughly for homogenization, and transferring it to the feed tank.

Next, The feed solution of  $\text{NaNO}_3$  is pumped through the column at a flow rate of 50-80 L/h. Exit flow and conductivity were recorded automatically. The process continued until an S-shaped curve was observed in the conductivity.

Finally, 10 L of water is pumped through the system and column to remove any  $\text{NaNO}_3$  in the mobile phase.

During all operations, the operator must manually adjust flow rates and the water height inside the column by adjusting valve V3. This is to ensure the resin is always submerged, and to limit excess water in the column.

### 2.3 Modelling

To describe the ion-exchange chromatography process, the Lumped Rate Model (LRM) with the Steric Mass Action (SMA) was used. The LRM and the SMA isotherm are given for each component  $i \in \{1, \dots, N_c\}$  in eq. (1)-(2).

$$\frac{\partial c_i}{\partial t} = D_{\text{ax}} \frac{\partial^2 c_i}{\partial z^2} - u \frac{\partial c_i}{\partial z} - \frac{1-\varepsilon}{\varepsilon} \frac{\partial q_i}{\partial t}, \quad (1)$$

$$\frac{\partial q_i}{\partial t} = k_{\text{kin},i} (k_{\text{eq},i} c_i \bar{q}_0 - q_i c_0^v). \quad (2)$$

Here,  $t$  is time,  $c_i$  is the mobile phase concentration of component  $i$ ,  $q$  is the corresponding stationary phase concentration,  $z$  is the spatial coordinate,  $D_{\text{ax}}$  is the axial dispersion coefficient,  $\varepsilon$  is the total porosity,  $k_{\text{eq}}$  is the equilibrium adsorption constant,  $k_{\text{kin}}$  is a kinetic constant,  $\bar{q}_0 = q_0 - \sum_j^{N_c} \sigma_j q_j$  is the number of free binding sites where  $q_0$  is the bound salt concentration and  $\sigma$  is the steric hindrance factor. The bound salt concentration is given by electroneutrality as  $q_0 = \Lambda - \sum_j^{N_c} v_j q_j$  where  $\Lambda$  is the ionic capacity and  $v$  is the characteristic charge. The boundary conditions are given in eq. (3)-(4), respectively.

$$u c_{\text{in},i} = u c_i(t, 0) - D_{\text{ax}} \frac{\partial c_i(t, 0)}{\partial z}, \quad (3)$$

$$\frac{\partial c_i(t, L)}{\partial z} = 0, \quad (4)$$

where  $L$  is the column length and  $c_{\text{in}}$  is the inlet concentration. If assuming isotherm equilibrium, the equations eq. (1)-(2) must be discretized and solved as a differential algebraic equations system, setting eq. (2) equal to 0. Alternatively, one can set a large  $k_{\text{kin}}$  value to approximate the equilibrium and still discretize and solve the system as an ordinary differential equation (ODE) system [4]. To solve the PDEs in eq. (1)-(4), the spatial domain of eq. (1) was discretized using the Discontinuous Galerkin Spectral Element Method (DGSEM) derived by Breuer et al [5]. The resulting system of ODEs was solved using the QNDF solver which is a stiff backwards differentiation formula solver using DifferentialEquations.jl [6,7].

#### Column Characterization

To model the pilot-scale ion exchange fixed-bed column, CADET-Julia was used [4]. In Table 1, all values

used for simulating the ion exchange system can be seen. The system was represented as three serially connected segments: the in-flow pipes, the ion exchange column itself, and the out-flow pipes. In Figure 1, this segmentation can be seen with respect to the physical system. Approximate measurements of pipe length and radii were used for the in-flow and out-flow sections. For the simulation, the value of the axial diffusion coefficient in the pipes,  $D_{\text{ax, pipes}}$ , was set to  $10^{-3} \text{ m}^2/\text{s}$ . This value was heuristically chosen to balance minimizing diffusion in the pipes while avoiding an excessively stiff system that would significantly increase the computational time.

For each batch, the median flow rate was calculated and applied as a constant flow in the simulated runs. The median flow was chosen to make the data cleaning more robust towards transmitted values that were deemed outliers. In some cases, pump start-ups were modelled by fitting flow profiles with second- or third-order polynomials, before transitioning to a constant flow profile.

The historical data of the washes were used to characterize the axial diffusion coefficient,  $D_{\text{ax}}$ , and resin porosity,  $\varepsilon$ . Parameter estimation was done by fitting a single value of  $D_{\text{ax}}$  and a single value of  $\varepsilon$  across all batches, ensuring they remain constant. Conductivity was converted to concentration by assuming the initial and final conductivity corresponded to concentrations of 0.1 and 0 N  $\text{NaNO}_3$ , respectively.

**Table 1:** Overview of variables used in simulation of the ion-exchange fixed-bed column using CADET-Julia.

Symbol	Description	Value Used
$L_{\text{pipes, in}}$	In-flow pipes length	6.74 m
$L_{\text{pipes, out}}$	Out-flow pipes length	0.19 m
$L$	Fixed-bed column length	0.095 m
$r_{\text{pipes}}$	Pipe radius	0.005 m
$r_{\text{column}}$	Column radius	0.055 m
$D_{\text{ax, pipes}}$	Axial diffusion coefficient in the pipes	$10^{-3} \text{ m}^2/\text{s}$
$\sigma_{\text{H}^+}/\sigma_{\text{Na}^+}$	Shielding factor	0 / 0
$v_{\text{H}^+}/v_{\text{Na}^+}$	Characteristic charge	1 / 1
$k_{\text{kin}}$	Kinetic coefficient	$10^8$

Subsequently, historical breakthrough curve data were used to fit the SMA model parameters: the ionic capacity,  $\Lambda$ , and the equilibrium coefficient,  $k_{\text{eq}}$ . Parameter estimation was done by fitting a single value of  $\Lambda$  and a single value of  $k_{\text{eq}}$  across all batches, ensuring they remain constant.

The ParticleSwarm algorithm from the Optim.jl package was utilized to perform global parameter searches, using the mean absolute error between simulated runs and historical data as the optimization metric [9].

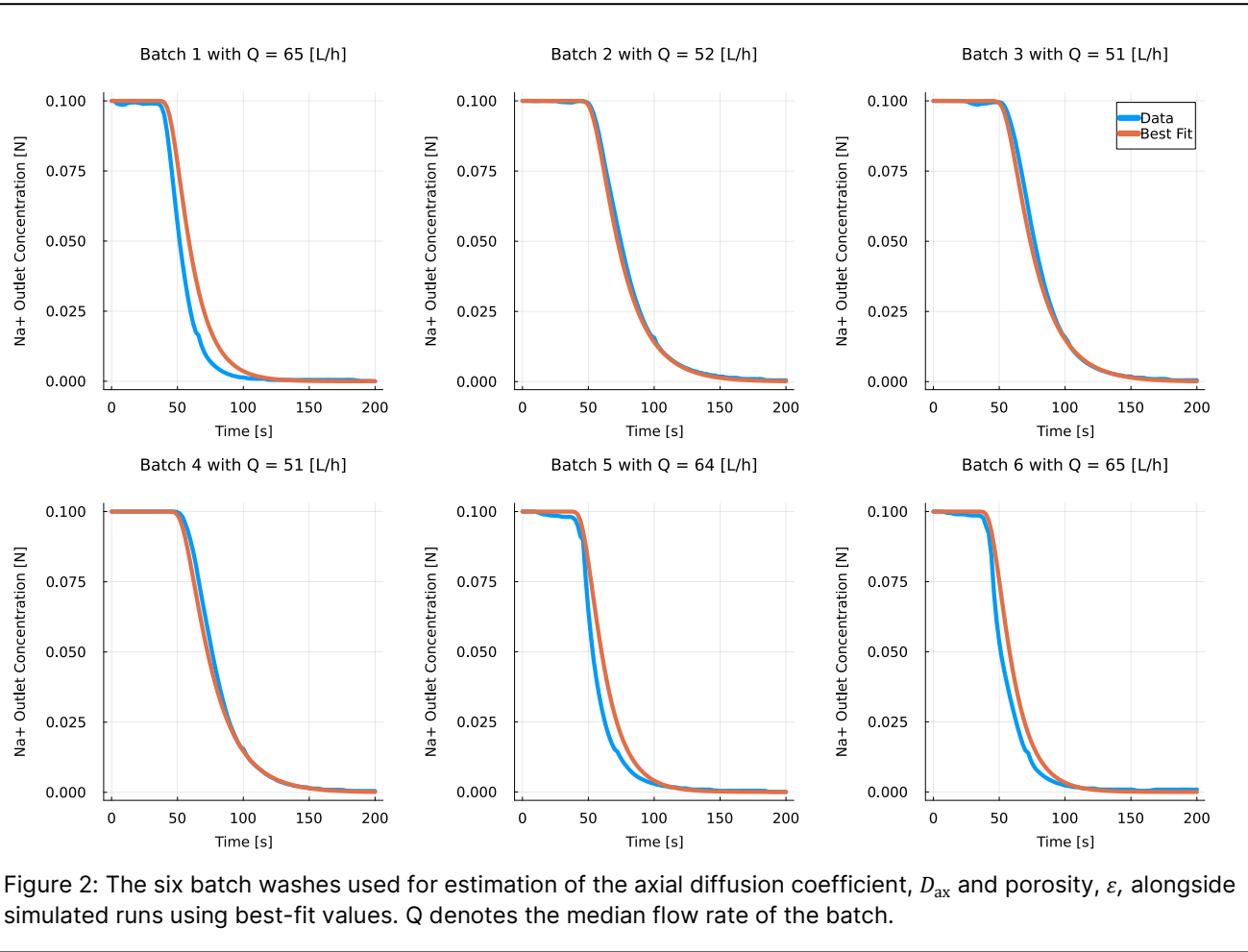


Figure 2: The six batch washes used for estimation of the axial diffusion coefficient,  $D_{ax}$  and porosity,  $\varepsilon$ , alongside simulated runs using best-fit values. Q denotes the median flow rate of the batch.

### 3. RESULTS & DISCUSSION

#### 3.1 Parameter Estimation

The batches of wash data were analyzed to estimate the best-fit values for the  $D_{ax}$  and  $\varepsilon$ , which were determined to be  $7 \times 10^{-5} \text{ m}^2/\text{s}$  and 0.6, respectively. Using these parameter values, Figure 2 illustrates the experimental wash curves alongside their simulated counterparts.

Subsequently, the SMA isotherm parameters  $\Lambda$  and  $k_{eq}$  were estimated from breakthrough data, which yielded values of 4 eq/L and 3, respectively. Figure 3 presents the experimental breakthrough curves and corresponding simulations.

The LRM with SMA isotherm produces strong fits for both wash data and the breakthrough data. The simulations predict the timing of the initial break of the curve well and follow the same evolution as the observed data.

#### Discussion

In Figure 2 and Figure 3, it can be observed that the simulations predict a delayed breakthrough when flow rates (Q) are higher, i.e.  $Q \approx 65 \text{ L/h}$ , compared to those

with lower flow rates, i.e.  $Q \approx 51 \text{ L/h}$ . This indicates there may be some flow-dependent mechanisms present in the process not entirely explained by the LRM model.

Discrepancies between the simulated and experimental results may stem from uncertainties in the historical data and inconsistent execution across batches. Variations in how operators controlled the water height in the column could have affected the observed conductivity. Additionally, the exact concentration of the  $\text{NaNO}_3$  solution is unknown; the concentration 0.1 N  $\text{NaNO}_3$  is assumed based on the exercise instructions. Furthermore, measurement uncertainties in the flow meter and conductivity sensors further contribute to discrepancies between historical data and simulations.

When preprocessing the data, it was observed that parameter estimation was highly sensitive to the choice of  $t = 0$ , defined as when flow from the feed tank to the column begins. As  $t = 0$  was not always clearly discernible, in some batches, it was approximated based on other batches where it was easier to identify. Horizontal translations of the wash curves significantly affected the converged values of the parameter estimation process.

The quality of the available datasets varied noticeably when evaluating historical data for parameter

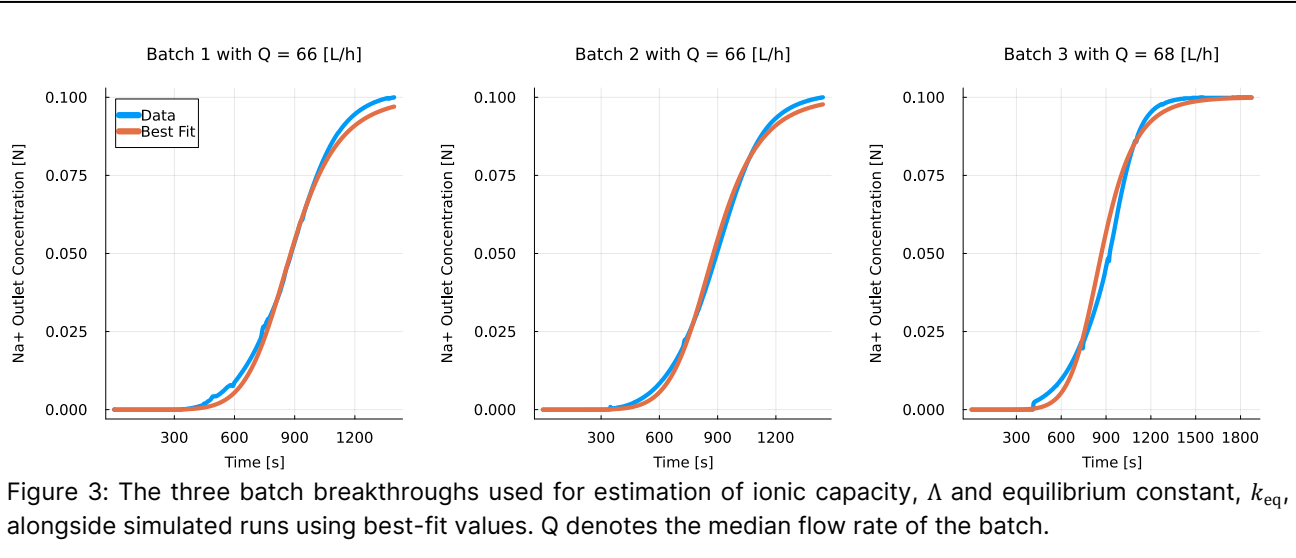


Figure 3: The three batch breakthroughs used for estimation of ionic capacity,  $\Lambda$  and equilibrium constant,  $k_{eq}$ , alongside simulated runs using best-fit values. Q denotes the median flow rate of the batch.

estimation. Smooth, undisrupted runs were critical to enabling parameter estimation. In this regard, some historical datasets were not considered for parameter estimation, and those used had to be preprocessed to make modeling feasible. The datasets most applicable to parameter estimation were those run by experienced operators conducting experiments for their research. "Data gathered by first-time operators often exhibited signs of process disruption and were rarely as directly usable for parameter estimation, compared to data produced with dedication to the purpose.

### 3.2 Computational Efficiency

In this study, the PDEs described in eqs. (1)–(4) were solved efficiently using DGSEM in CADET-Julia. On an i5-1345U processor (1.60 GHz), the equations were discretized and solved in under two seconds, below the measurement frequency. This was true for both the wash data, each consisting of approximately 100 data points, and the breakthrough data, containing up to 1000 points.

The global parameter searches for all washes and breakthroughs were completed in less than 10 minutes each. Notably, accounting for the inherent uncertainties in the system, adequate parameter values were identified already within the first 1–2 minutes. Additional search iterations refined these values, but the improvements exceed the level of accuracy achievable given the uncertainties present.

### Discussion

The ability to solve the LRM with the SMA isotherm within the 2-second measurement frequency showcases the model's potential for real-time computer-aided applications. In its current state, the model can predict breakthrough profiles at a speed that enables it to be deployed in real-time. By connecting the model to live data feeds of the flow in the column, the model can alter its predicted breakthrough profile for every new data point.

Currently, the model predicts the entire breakthrough profile from  $t = 0$  to the end of the data series, up to some 30 minutes in the future. The computation time can be further reduced by optimizing the routine to avoid redundant calculation on already-past data. The prediction horizon can also be limited, and more powerful hardware can be used to perform calculations.

This may bring the computation time below one second, and effort could then be spent in reducing the sensor measurement frequency to similarly match that. This naively ignores any time taken to retrieve data from the system.

The global parameter search can currently be completed in 1–10 minutes. To further accelerate this, an approach could be employing a local search algorithm with a well-informed initial guess. With tactics like this, the parameter estimation procedure could be reduced to sub-minute computation times.

This may enable real-time parameter adjustment, allowing the system to dynamically adapt to batch-to-batch variations. While it makes little sense for variables like,  $D_{ax}$ ,  $\varepsilon$ ,  $k_{eq}$ , or  $\Lambda$  to change between batches, other parameters could be introduced to explain the effects of operating conditions and batch-to-batch variation.

### 3.3 Perspectives

The developed tool can be implemented directly to approximate breakthrough duration during operation. By evaluating the model in real-time, operators can see the impact of adjusting flow on the breakthrough profile.

To enhance the modeling capabilities demonstrated in this study, additional metadata on the process would be beneficial. Specifically, this includes:

- Timestamps for  $t = 0$  as the precise point when all the flow from the T1 feed tank is directed into the column.

- Measured concentrations of the NaNO<sub>3</sub> solution used for breakthrough.
- Some indication of the operator's ability to maintain the water height within the column.

These lacking metadata mirror challenges frequently faced in industrial systems, where incomplete metadata, missing signals, and absent critical sensors hinder effective modeling.

The investigation has demonstrated the feasibility of characterizing pilot-scale equipment from historical data that mirrors industrial operational data. The methods employed here can be applied to historical data from industrial systems. Using fast numerical schemes or other methods, real-time computer-aided process insights and predictions could be granted to process operators. Parameter search optimizations can be employed for real-time determination of factors that vary from batch to batch.

The approach adopted in this study—leveraging historical data to identify areas of improvement—provides a framework for addressing these challenges. Drawing a clear connection between historical data and its value in developing real-time applications makes it possible to prioritize investments in metadata collection, new sensors, or dsata processing tools. These investments would provide a return in the improved ability to conduct real-time decision-making during operation to increase product yield.

Additional historical data and process understanding could be used to monitor the long-term health and efficiency of the system. In the case of ion-exchange, it could be used to quantify resin degradation and better schedule replacements.

## 4. CONCLUSION

This study demonstrates the potential for real-time analysis of ion-exchange chromatography using historical pilot-scale data of a fixed-bed ion exchange column. Despite challenges such as incomplete metadata and variability in manual operations, the findings confirm that the system can be accurately characterized using only operational historical data

By employing fast computational techniques, the study shows that the system can be modeled in real time, simulating entire breakthrough profiles within the two-second measurement frequency of the system. These findings underscore the potential of using historical data to develop valuable real-time computer-aided process applications in pilot and industrial-scale settings.

## ACKNOWLEDGEMENTS

The authors of this work acknowledge the efforts of

students and staff at courses in experimental unit operations at the Department of Chemical and Biochemical Engineering for making data. Additionally, the authors would like to express gratitude to the Novo Nordisk Foundation for their support for the digital infrastructure of pilot facilities through grant NNF19SA0035474.

## REFERENCES

1. Kozorog M, et al. Model-based process optimization for mAb chromatography. *Sep Purif Technol* 2023;305:122528.
2. Kumar V, and and Lenhoff AM. Mechanistic Modeling of Preparative Column Chromatography for Biotherapeutics. *Annu Rev Chem Biomol Eng* 2020;11:235–55.
3. Jones MN et al. Pilot Plant 4.0: A Review of Digitalization Efforts of the Chemical and Biochemical Engineering Department at the Technical University of Denmark (DTU). *Comput. Aided Chem. Eng.*, vol. 49, Elsevier; 2022, p. 1525–30.
4. Frandsen J, et al. CADET-Julia: Efficient and versatile, open-source simulator for batch chromatography in Julia. *Comput Chem Eng* 2025;192:108913.
5. Breuer JM, et al. Spatial discontinuous Galerkin spectral element method for a family of chromatography models in CADET. *Comput Chem Eng* 2023;177:108340.
6. Shampine LF, and Reichelt MW. The MATLAB ODE Suite. *SIAM J Sci Comput* 1997;18:1–22.
7. Rackauckas C, and Nie Q. DifferentialEquations.jl – A Performant and Feature-Rich Ecosystem for Solving Differential Equations in Julia. *J Open Res Softw* 2017;5:15.
8. Large-Scale Exercises in Process Technology and Chemical Unit Operations. Danish Technical University, Department of Chemical and Biochemical Engineering, Pilot Plant; 2024.
9. K Mogensen P, and N Riseth A. Optim: A mathematical optimization package for Julia. *J Open Source Softw* 2018;3:615.

© 2025 by the authors. Licensed to PSEcommunity.org and PSE Press. This is an open access article under the creative commons CC-BY-SA licensing terms. Credit must be given to creator and adaptations must be shared under the same terms. See <https://creativecommons.org/licenses/by-sa/4.0/>

